Received: 22 April 2019 | Accepted: 22 August 2019

DOI: 10.1111/gcb.14816

PRIMARY RESEARCH ARTICLE

Global Change Biology WILEY

Global vegetation biomass production efficiency constrained by models and observations

Yue He[1] | Shushi Peng[1] | Yongwen Liu[1,2,3] | Xiangyi Li[1] | Kai Wang[1] | Philippe Ciais[4] | M. Altaf Arain[5] | Yuanyuan Fang[6] | Joshua B. Fisher[7] | Daniel Goll[4] | Daniel Hayes[8] | Deborah N. Huntzinger[9] | Akihiko Ito[10,11] | Atul K. Jain[12] | Ivan A. Janssens[13] | Jiafu Mao[14] | Campioli Matteo[13] | Anna M. Michalak[6] | Changhui Peng[15,16] | Josep Peñuelas[17,18] | Benjamin Poulter[19] | Dahe Qin[20,21] | Daniel M. Ricciuto[14] | Kevin Schaefer[22] | Christopher R. Schwalm[23,24] | Xiaoying Shi[15] | Hanqin Tian[25] | Sara Vicca[13] | Yaxing Wei[14] | Ning Zeng[26] | Qiuan Zhu[15,16]

[1]Sino-French Institute for Earth System Science, College of Urban and Environmental Sciences, Peking University, Beijing, China

[2]Key Laboratory of Alpine Ecology, Institute of Tibetan Plateau Research, Chinese Academy of Sciences, Beijing, China

[3]CAS Center for Excellence in Tibetan Earth Science, Chinese Academy of Sciences, Beijing, China

[4]Laboratoire des Sciences du Climat et de l'Environnement, CEA CNRS UVSQ, Paris, France

[5]School of Geography and Earth Sciences and McMaster Centre for Climate Change, McMaster University, Hamilton, ON, Canada

[6]Department of Global Ecology, Carnegie Institution for Science, Stanford, CA, USA

[7]Jet Propulsion Laboratory, California Institute of Technology, Pasadena, CA, USA

[8]School of Forest Resources, University of Maine, Orono, ME, USA

[9]School of Earth Sciences and Environmental Sustainability, Northern Arizona University, Flagstaff, AZ, USA

[10]National Institute for Environmental Studies, Tsukuba, Japan

[11]Japan Agency for Marine-Earth Science and Technology, Yokohama, Japan

[12]Department of Atmospheric Sciences, University of Illinois, Urbana, IL, USA

[13]Centre of Excellence PLECO (Plant and Vegetation Ecology), Department of Biology, University of Antwerp, Wilrijk, Belgium

[14]Environmental Sciences Division and Climate Change Science Institute, Oak Ridge National Laboratory, Oak Ridge, TN, USA

[15]Institute of Environment Sciences, Biology Science Department, University of Quebec at Montreal, Montreal, QC, Canada

[16]State Key Laboratory of Soil Erosion and Dryland Farming on the Loess Plateau, College of Forestry, Northwest A & F University, Yangling, China

[17]CSIC, Global Ecology Unit CREAF-CEAB-UAB, Barcelona, Spain

[18]CREAF, Barcelona, Spain

[19]Institute on Ecosystems and the Department of Ecology, Montana State University, Bozeman, MT, USA

[20]State Key Laboratory of Cryospheric Sciences, Northwest Institute of Eco-environment and Resources, Chinese Academy of Sciences, Lanzhou, China

[21]National Climate Center, China Meteorological Administration, Beijing, China

[22]National Snow and Ice Data Center, University of Colorado, Boulder, CO, USA

[23]Woods Hole Research Center, Falmouth, MA, USA

[24]Center for Ecosystem Science and Society, Northern Arizona University, Flagstaff, AZ, USA

[25]International Center for Climate and Global Change Research and School of Forestry and Wildlife Sciences, Auburn University, Auburn, AL, USA

[26]Department of Atmospheric and Oceanic Science, University of Maryland, College Park, MD, USA

Correspondence
Shushi Peng, Sino-French Institute for Earth System Science, College of Urban and Environmental Sciences, Peking University, Beijing 100871, China.
Email: speng@pku.edu.cn

Funding information
National Natural Science Foundation of China, Grant/Award Number: 41671079, 41701089 and 41722101; National Key Research and Development Program of China, Grant/Award Number: 2016YFA0600202 and 2016YFC0500203; H2020 European Research Council, Grant/Award Number: ERC-2013-SyG-610028

Abstract

Plants use only a fraction of their photosynthetically derived carbon for biomass production (BP). The biomass production efficiency (BPE), defined as the ratio of BP to photosynthesis, and its variation across and within vegetation types is poorly understood, which hinders our capacity to accurately estimate carbon turnover times and carbon sinks. Here, we present a new global estimation of BPE obtained by combining field measurements from 113 sites with 14 carbon cycle models. Our best estimate of global BPE is 0.41 ± 0.05, excluding cropland. The largest BPE is found in boreal forests (0.48 ± 0.06) and the lowest in tropical forests (0.40 ± 0.04). Carbon cycle models overestimate BPE, although models with carbon–nitrogen interactions tend to be more realistic. Using observation-based estimates of global photosynthesis, we quantify the global BP of non-cropland ecosystems of 41 ± 6 Pg C/year. This flux is less than net primary production as it does not contain carbon allocated to symbionts, used for exudates or volatile carbon compound emissions to the atmosphere. Our study reveals a positive bias of 24 ± 11% in the model-estimated BP (10 of 14 models). When correcting models for this bias while leaving modeled carbon turnover times unchanged, we found that the global ecosystem carbon storage change during the last century is decreased by 67% (or 58 Pg C).

KEYWORDS
biomass production, BPE, carbon sink, emergent constraint, terrestrial biosphere model

1 | INTRODUCTION

Biomass production (BP) consists of photosynthetically derived carbon used for biomass growth, that is, to build up leaves, wood, and roots (Vicca et al., 2012). BP is smaller than net primary productivity (NPP), which is the sum of BP and carbon allocated to nonstructural organic compounds that are used to maintain functions of rhizosphere and plant (e.g., mycorrhizae, root exudates, and volatile carbon compound emissions; Campioli et al., 2015; Chapin et al., 2006; Vicca et al., 2012). A large fraction of BP (about 8.2 Pg C/year) is being appropriated by humans through the harvest of food, wood, and fibers (Erb et al., 2016; Haberl et al., 2007). The remaining BP enters into a cascade of ecosystem carbon pools, and determines the land carbon balance (Friend et al., 2014). Currently, nonharvested BP forces a carbon sink offsetting one-third of anthropogenic emissions (Le Quéré et al., 2015). The fate of this carbon sink, however, is highly uncertain under climate change and anthropogenic activities (Ciais et al., 2013; Peñuelas et al., 2017). In particular, since BP is a fraction of photosynthetically assimilated carbon (gross primary production, GPP), both dynamics in GPP and the fraction of GPP allocated to BP could affect the outcome of BP.

Progress has been made to derive observation-based GPP estimates from eddy covariance networks (Beer et al., 2010), and from new remote sensing data (e.g., solar-induced chlorophyll fluorescence, Guanter et al., 2014; near-infrared reflectance of vegetation, Badgley, Field, & Berry, 2017). However, we still know little about the allocation of GPP to BP, hereafter defined as biomass production efficiency (BPE), that is, the ratio of BP to GPP. This is because in situ estimates of BP are rarely at the same locations as GPP. Earlier studies usually suggest a constant BPE universally (Gifford, 1995; McCree & Troughto, 1966; Waring, Landsberg, & Williams, 1998). However, more recent syntheses of both field measurements and remote sensing products all indicate that BPE varies greatly across vegetation types, environmental conditions, ecosystem management intensity, and soil fertility gradients (Campioli et al., 2015; Fernández-Martínez et al., 2014; Vicca et al., 2012; Zhang, Xu, Chen, & Adams, 2009; Zhang et al., 2014). This spatial heterogeneity of BPE hinders the upscaling of this quantity to a global scale.

Terrestrial carbon cycle models simulate the dynamics of CO_2 fluxes and carbon pools in response to variations in climate and atmospheric composition, and can be run with climate scenarios to project future carbon storage change (Cramer et al., 2001; Friedlingstein et al., 2006; Piao et al., 2008; Yao, Piao, & Wang, 2018). Previous models often assumed a constant fraction of autotrophic respiration (R_a) to GPP as a simplifying concept (e.g., Landsberg & Waring, 1997; Nemani et al., 2009; Sands, Battaglia, & Mummery, 2000; Veroustraete, Sabbe, & Eerens, 2002), whereas ecosystem models at present employ more detailed descriptions of the carbon cycle (e.g., Krinner et al., 2005; Peng, Liu, Dang, Apps, & Jiang, 2002; Tian et al., 2012; Zhu et al., 2014). These latter carbon cycle models have structural similarities in the equations of leaf scale photosynthesis (Rogers et al., 2017) and soil carbon dynamics (Luo et al., 2016), but they differ

greatly regarding how GPP assimilates are allocated to different plant organs or respired for maintenance and growth purposes, the processes that determine BPE. In this respect, BPE in a model is not a parameter, but rather a diagnostic variable that can be calculated from model outputs and reflects plant processes driven by environmental conditions and ecological stoichiometry in the case of models integrating carbon–nutrient interactions. Note that in current models, BP = NPP, because mycorrhizae and exudates are not considered.

In this study, we aim to quantify the global value of BPE by applying an emergent constraint approach (Cox et al., 2013; Kwiatkowski et al., 2017; Wenzel, Cox, Eyring, & Friedlingstein, 2014; Zhao et al., 2016) to model outputs from a recent dataset of BPE measured globally (Campioli et al., 2015). This approach can reduce the intermodel uncertainties by identifying a robust linear intermodel relationship between one quantity that cannot be directly measured and the other quantity with available field observations. When combined with observations of the second quantity, this relationship can be used to constrain the first quantity (see Materials and Methods). The set of global carbon cycle models we used is known as the Multi-scale Synthesis and Terrestrial Model Intercomparison Project (MsTMIP; Huntzinger et al., 2013; Wei et al., 2014; see model list in Table S1). We also extend this analysis to an evaluation of the model performance in simulating global BP, and ecosystem carbon storage change during 1901–2010, with a distinction between carbon-only and carbon–nitrogen interactions.

2 | MATERIALS AND METHODS

2.1 | BPE datasets

The newly assembled BPE dataset developed by Campioli et al. (2015) contains 131 field observations, including forests, grasslands, croplands, wetlands, and tundra. For the current study, 18 sites were excluded because carbon cycle models do not have an explicit consideration of wetlands and tundra at present. In total, 113 observation-based BPE values covering almost all major vegetation types were obtained, including 33 data points of boreal forests (BoF), 31 data points of temperate forests (TeF), five data points of tropical forests (TrF), 20 data points of grasslands, and 24 data points of croplands.

A binary management classification scheme was also adopted in our study (Campioli et al., 2015). This classification scheme contained both managed status (when the site was dominated by human activity, such as thinning, harvesting, or planting for forests, or newly established and fertilized grasslands) and unmanaged status (when the site was dominated by natural processes with a low human activity impacts). The anthropogenic ecosystem, that is, cropland, is inherently under managed conditions. This BPE dataset also contained information of site fertility, which was divided into three levels (i.e., low, medium, or high nutrient availability), according to information in previous studies or provided by associated authors (Campioli et al., 2015). In addition, climate data (i.e., mean annual temperature and mean annual precipitation) for each site were retrieved from the WorldClim database (http://worldclim.org/version2; Fick & Hijmans, 2017).

The uncertainty ranges of BP and GPP for each site were estimated based on method-specific reduction factor determined by expert judgment, the number of measurement years, and vegetation type (Campioli et al., 2015; Luyssaert et al., 2007). Campioli et al. (2015) calculated the uncertainty range of BPE for each site by the means of the error propagation theory. And we then used this error propagation method to obtain the statistical uncertainty of averaged BPE across all sites (e.g., the red shaded area shown in Figure 1a represents the uncertainty range of site-level mean BPE).

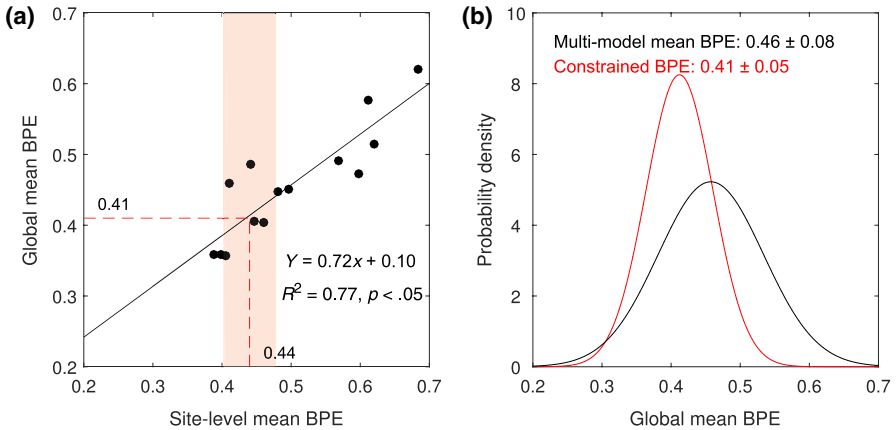

FIGURE 1 Emergent constraint on the global mean biomass production efficiency (BPE). (a) Relationship between the modeled global (excluding cropland) and site-level mean BPE of unmanaged vegetation. The black line represents the best fit across different models (black dots), the vertical red dashed line and shaded area represent the mean value of BPE and its statistical uncertainty from field observations, respectively (see Materials and Methods), and the horizontal red dashed line represents the constrained global mean BPE. (b) Probability density function for global BPE. The black line represents the probability distribution of the multimodel mean BPE, assuming that all BPE values estimated from terrestrial carbon models conform to a Gaussian distribution, the red line represents the probability distribution of global BPE constrained by field observations, and the black and red letters represent the values of global BPE (mean ± standard deviation) before and after the field constraints, respectively

2.2 | GPP datasets

We used three different data-driven GPP datasets in our study, as they are often considered as benchmark for model evaluation (Li et al., 2019; Piao et al., 2013). The first one is an eddy covariance flux tower data-driven GPP product at a spatial resolution of 0.5° during 1982–2011 (Jung et al., 2011). The second one is Moderate Resolution Imaging Spectroradiometer (MODIS) GPP product (collection 055) at 1 km resolution over 2000–2012 (Zhao, Heinsch, Nemani, & Running, 2005). The third one is derived from a process-based model, the Breathing Earth System Simulator with a spatial resolution of 1 km over 2000–2015 (Jiang & Ryu, 2016). Here, all these GPP datasets were regridded to a common 0.5° grid to match the carbon cycle models used in our study. We separately calculated the mean annual global GPP during their observation period, and the average of them was further used in the calculation of global BP (excluding cropland).

2.3 | Carbon cycle models

We used modeling results from the Multi-scale Synthesis and Terrestrial Model Intercomparison Project (MsTMIP; Huntzinger et al., 2013; Wei et al., 2014) to calculate model-derived BPE. All model simulations participating in this project were performed with the same protocol for the period of 1901–2010 and at a 0.5° spatial resolution. Here, we focused on model outputs over the past three decades (1981–2010) from the "SG3" simulation, which was forced with time-varying climate, atmospheric CO_2 concentrations, and land use and land-cover change. A total of 14 models drawn from MsTMIP version 1 (http://dx.doi.org/10.3334/ORNLDAAC/1225) were used in this study. These 14 MsTMIP models are CLASS-CTEM-N, CLM4, CLM4VIC, DLEM, GTEC, ISAM, LPJ-wsl, ORCHIDEE-LSCE (ORCHIDEE hereafter), SiB3, SiBCASA, TEM6, TRIPLEX-GHG, VEGAS2.1, and VISIT (see Table S1). These 14 MsTMIP models were further divided into two groups based on whether an explicit nitrogen cycling was considered in each model, namely models with carbon–nitrogen interactions (CLASS-CTEM-N, CLM4, CLM4VIC, DLEM, ISAM, TEM6, TRIPLEX-GHG) and models without carbon–nitrogen interactions (GTEC, LPJ-wsl, ORCHIDEE, SiB3, SiBCASA, VEGAS2.1, VISIT). The direct outputs of four variables, that is, the NPP, GPP, total living biomass, and total soil carbon were used in this analysis. Because TRIPLEX-GHG did not report the NPP data in the MsTMIP variable list online, we calculated NPP indirectly as the difference between GPP and R_a for this model. To estimate the changes in modeled carbon storage, three models were excluded for reasons being either unavailability of carbon pools (SiB3) or nonphysical values of soil carbon stocks (CLASS-CTEM-N and CLM4VIC) due to issue such as nonlinear interactions among hydrologic and carbon cycle parameters (Huang et al., 2016; Sargsyan et al., 2014). In MsTMIP, NPP equals BP as all carbon cycle models do not deal with nonstructural NPP components (e.g., root exudation and root symbionts) explicitly at present. Thus, the modeled NPP is hereafter called modeled BP in our study.

All of the global land cover maps used in MsTMIP models originated from the Synergetic Land Cover Product (SYNMAP; Jung, Henkel, Herold, & Churkina, 2006; Wei et al., 2014). To be compatible with the five vegetation types adopted by this study, the 47 SYNMAP classes (excluding shrubs, snow, barren, and urban areas) used in SYNMAP were first reclassified into three plant functional types (PFTs; i.e., forests, grasslands, and croplands) based on a translation method defined by Jung et al. (2006). Here, croplands included all those SYNMAP vegetation classes with "crops" as a life form. According to the Köppen–Geiger climate classification (Peel, Finlayson, & McMahon, 2007), the forests located in boreal/tropical regions were then merged into BoF/TrF, while those over temperate areas were renamed as TeF. Using this reconstructed land cover map, represented PFT was defined as the PFT covering more than 50% of the fractional area in each grid cell. To obtain global natural vegetation BP and GPP, the grid cells with cropland as represented PFT were excluded in the calculation.

2.4 | Model constraining

We further adopted the recently widely used "emergent constraint" approach (e.g., Cox et al., 2013; Kwiatkowski et al., 2017; Wenzel et al., 2014; Zhao et al., 2016) to reduce the uncertainties in MsTMIP-simulated global mean BPE. This approach relies on a strong linear intermodel relationship between one quantity that cannot be directly measured and the other quantity with available field observations. A more accurate estimate can be achieved by constraining the first quantity through available field observations of the second quantity (illustrated schematically in the box 1 from Eyring et al., 2019). Here, using a similar method like Zhao et al. (2016), we first built a linear relationship between global and site-level mean BPE values across the 14 MsTMIP models (as shown in Figure 1a). This model-derived relationship between global and site-level mean BPE, combined with field observations, provided an emergent constraint on the simulated global mean BPE. Specifically, the conditional probability density function (PDF) for the constrained global BPE was calculated by integrating the PDF of the observations with the PDF of the model-derived regression line. More detailed information of the "emergent constraint" approach can be found in Appendix S1.

We first computed the values of site-level BPE from modeled BP and GPP at the same location and for the same vegetation type than observed data. We only used BPE data from 83 unmanaged sites (except for cropland) because forest and grassland management was not taken into account in the MsTMIP models. As cropland management is not well represented in current models with simplified and incomplete description (Piao et al., 2018), the cropland sites are not included in the emergent constraint for the global mean BPE, while they are included for the vegetation type level BPE only for comparison. We also excluded 28 sites because their vegetation type was a fraction smaller than 50% of the modeled vegetation in the corresponding grid cell (hereafter these data are called nonrepresentative data). This leaves 55 sites for our analysis, including 36 non-cropland sites. Hence, the constraining approach was applied to all PFTs combined (Figure 1,

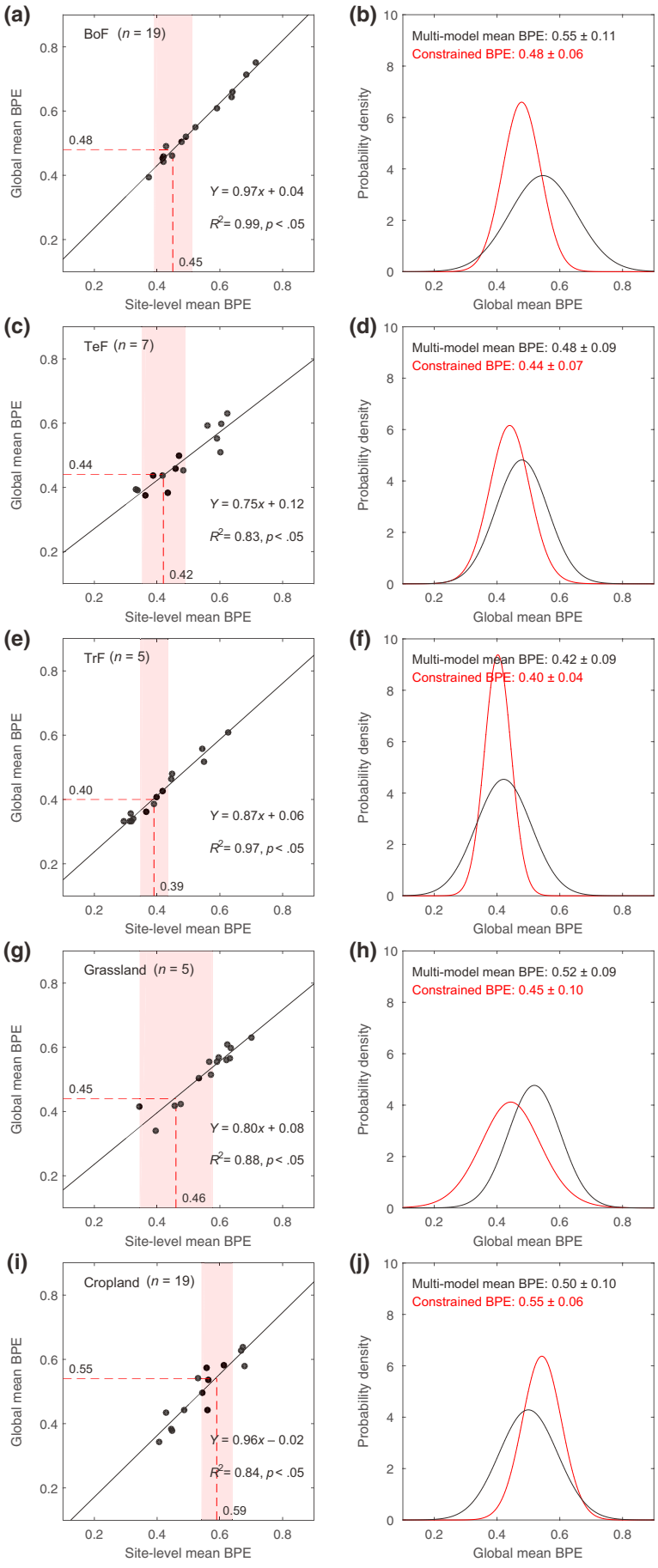

FIGURE 2 Emergent constraint on the mean biomass production efficiency (BPE) for different vegetation types. Same as Figure 1 but the field observations are divided into five vegetation types: (a, b) Boreal forests (BoF). (c, d) Temperate forests (TeF). (e, f) Tropical forests (TrF). (g, h) Grassland. (i, j) Cropland. Only unmanaged observations (except for cropland) for which the fraction of their represented vegetation type is higher than 50% of area in the corresponding model pixel are included. Right-hand column shows the relationship between modeled biome-specific and site-level mean BPE across 14 MsTMIP models, for five vegetation types, respectively. In each panel, *n* is the sample size of the field observations, the black line represents the best fit across different models (black dots), the vertical red dashed line and shaded area represent the mean value of BPE and its statistical uncertainty from field observations, respectively, and the horizontal red dashed line represents the constrained mean BPE. Left-hand column shows the probability distributions of mean BPE across 14 MsTMIP models, for five vegetation types, respectively. In each panel, the black line represents the probability distribution of multimodel mean BPE, assuming that all BPE values estimated from terrestrial carbon models can be represented by a Gaussian distribution, the red line represents the probability distribution of global mean BPE constrained by field observations, and the black and red letters represent the values of BPE (mean ± standard deviation) before and after constraint, respectively

excluding cropland, n = 36) and to each individual PFT (Figure 2; Figures S3 and S4).

2.5 | Changes in global ecosystem carbon storage during 1901–2010

We used a total of 11 MsTMIP models (i.e., CLM4, DLEM, GTEC, ISAM, LPJ-wsl, ORCHIDEE, SiBCASA, TEM6, TRIPLEX-GHG, VEGAS2.1, and VISIT) "SG3" simulations with GPP, BP, soil carbon storage, and biomass carbon storage available. Based on the constrained global BPE, we further applied a two-box model (Liu et al., 2019) and re-estimated the changes in global (excluding cropland) ecosystem carbon storage during 1901–2010 for each model as following steps.

First, we calculated the turnover times of global ecosystem biomass carbon and soil carbon in each year during 1902–2010 for each model using the following equation set:

$$\begin{cases} \tau_B(i) = \frac{C_B(i)}{NPP(i) - \Delta C_B(i)} \\ K_B(i) = \frac{1}{\tau_B(i)} \\ \tau_S(i) = \frac{C_S(i)}{C_B(i) \times k_B(i) - \Delta C_S(i)} \\ K_S(i) = \frac{1}{\tau_S(i)}, \end{cases} \quad (1)$$

where, $C_B(i)$ is the biomass carbon storage in year i, $\Delta C_B(i)$ is the change in biomass carbon storage from year $i-1$ to year i [$\Delta C_B(i) = C_B(i) - C_B(i-1)$], NPP($i$) is the NPP in year i, $\tau_B(i)$ is the turnover time of biomass carbon in year i, $k_B(i)$ is the turnover rate of biomass carbon in year i, $C_S(i)$ is the soil carbon storage in year i, $\Delta C_S(i)$ is the change in soil carbon storage from year $i-1$ to year i [$\Delta C_S(i) = C_S(i) - C_S(i-1)$], $\tau_S(i)$ is the turnover time of soil carbon in year i, $k_S(i)$ is the turnover rate of soil carbon in year i, i is year during 1902–2010 (i = 2, 3, 4, …, 110).

Second, assuming that simulated carbon pools in 1901 are in equilibrium (Figure S6) and BPE is invariant during 1901–2010 (equals to, in numeral, the constrained BPE). The biomass (C'_B) and soil carbon (C'_S) storage in each model in 1901 were recalculated as $C'_B(1) = \mathrm{GPP}(1) \times \mathrm{BPE}_{\mathrm{Constrained}} \times \tau_B(1)$ and $C'_S(1) = \mathrm{GPP}(1) \times \mathrm{BPE}_{\mathrm{Constrained}} \times \tau_S(1)$, respectively. Here, $C'_B(1)$ and $C'_S(1)$ are the re-estimated biomass and soil carbon storage in each model in 1901, respectively. GPP(1) is the GPP in the first year (1901). $\mathrm{BPE}_{\mathrm{Constrained}}$ is the constrained global natural vegetation BPE (0.41). $\tau_B(1)$ is the turnover time of biomass carbon in the first year (1901), assuming that $\tau_B(1)$ equals $\tau_B(2)$ in Equation (1). $\tau_S(1)$ is the turnover time of soil carbon in the first year (1901), assuming that $\tau_S(1)$ equals $\tau_S(2)$ in Equation (1). Then, we reconstructed the global biomass carbon and soil carbon in each year during 1902–2010 for each model using the following equations:

$$\begin{cases} C'_B(i) - C'_B(i-1) = \mathrm{GPP}(i) \times \mathrm{BPE}_{\mathrm{constrained}} - C'_B(i) \times k_B(i) \\ C'_S(i) - C'_S(i-1) = C'_B(i) \times k_B(i) - C'_S(i) \times k_S(i), \end{cases} \quad (2)$$

where $C'_B(i)$ is the re-estimated biomass carbon storage in year i, GPP(i) is the GPP in year i, $\mathrm{BPE}_{\mathrm{Constrianed}}$ is the constrained global natural vegetation BPE (0.41), $k_B(i)$ is the turnover rate of biomass carbon in year i, $C'_S(i)$ is the re-estimated soil carbon storage in year i, $k_S(i)$ is the turnover rate of soil carbon in year i, i is year during 1902–2010 (i = 2, 3, 4, …, 110).

Last, we calculated the changes in global carbon storage (biomass carbon + soil carbon) during 1901–2010, using biomass and soil carbon storage in the original MsTMIP model outputs and re-estimated by Equation (2) separately. Paired t test was used to test the difference between original and reproduced global ecosystem carbon storage changes during 1901–2010.

3 | RESULTS

3.1 | Emergent constraint on the global mean BPE

Figure 1a shows the relationship between modeled global and site-level mean BPE (cropland is excluded throughout this section, see Materials and Methods). MsTMIP models simulate a large spread in global non-cropland BPE, with a range going from 0.36 for the TRIPLEX-GHG model to 0.62 for the SiB3 model (Figure 1a). We found a strong linear relationship across different models between their site-level and global mean BPE (R^2 = 0.77, p < .05). This allows us to define an emergent constraint relationship (see Materials and Methods; Cox et al., 2013; Kwiatkowski et al., 2017; Wenzel et al., 2014; Zhao et al., 2016) whereby the selected field observations can be used to constrain the global modeled value of BPE. According to the emerging relationship shown in Figure 1a and the average of selected field BPE observations (0.44), the constrained global best estimate of BPE is 0.41. It is lower than the original multimodel average (0.46). When compared to the unconstrained PDF of models (black line), the constrained PDF (red line) is more narrow, so that the uncertainty on BPE is reduced from ±0.08 to ±0.05 (1-σ *SD*, Figure 1b).

Given that several studies showed nutrient scarcity to be associated with lower BPE for comparable GPP level (Fernández-Matínez et al., 2014; Vicca et al., 2012), we divided the models into two groups, those with (n = 7) and without (n = 7) carbon–nitrogen interactions, to test possible controls of BPE by nutrient limitations. Result shows that the constrained global BPE and uncertainty range are almost the same between the two groups of models (0.40 ± 0.05 for models with carbon–nitrogen interactions and 0.41 ± 0.05 for the other models; Figure S1). Models with carbon–nitrogen interactions (0.47 ± 0.08) tend to better match site observations (0.44 ± 0.04) compared to carbon-only models (0.53 ± 0.09), because of their lower BPE (Figure S1). At the global scale, the BPE from models with carbon–nitrogen interactions (0.43 ± 0.07) is also smaller than that from carbon-only models (0.49 ± 0.08; Figure S1). This is consistent with a decrease of BPE observed at forest sites under nitrogen limitation (Vicca et al., 2012). Furthermore, the constrained global mean BPE for models with carbon–nitrogen interaction is robust when separately calculated using site-level BPE with different nutrient availability classes (categorized as low, medium, and high nutrient level; see Materials and Methods; Figure S2).

3.2 | Emergent constraint on the mean BPE for different vegetation types

Applying a similar emerging constraint method, we also constrained BPE for the different vegetation types, including forests, grasslands, and croplands (see Materials and Methods). To do so, we conventionally divided forest sites into boreal, temperate, and tropical groups (Campioli et al., 2015; Luyssaert et al., 2007). Strong linear relationships like the one in Figure 1 were also found within each vegetation type ($p < .05$, Figure 2) particularly for boreal and TrF, with $R^2 > 0.9$. The constrained BPE is substantially lower than the original multimodel average for each vegetation type, except cropland (Figure 2). A noticeable decrease of BPE (constrained value minus original model mean) is found in BoF (Figure 2a). The multimodel mean BPE for BoF is 0.55 ± 0.11, but the magnitude of BPE after the constraint from observations is decreased to 0.48 ± 0.06. In contrast, crops have a higher BPE when constrained by field observations (Figure 2e). The higher BPE for crops from observations (0.55 ± 0.06) than from models (0.50 ± 0.10) may be related to several traits and processes that are not included in models, including crop varieties and more generally the allocation processes specific to crop plant types, and management operations such as irrigation and fertilization. The sample sizes of the site data (n) used to constrain BPE in some vegetation types are small ($n = 5$), but the constrained values of BPE are robust even if we include nonrepresentative data (Figures S3), or if we base the site-level model estimates on all pixels with similar climate as the site observations instead of only the pixel of the actual site location (the difference in climate conditions within an interval of 1°C × 50 mm; Figures S4). Overall, among the natural vegetation types, the lowest value of BPE after applying the constraint is found for TrF (0.40 ± 0.04) and the largest is for BoF (0.48 ± 0.06; Table S2).

4 | DISCUSSION

4.1 | Possible reasons for overestimated BPE in models

As mentioned above, BPE can be used as a critical diagnostic parameter to characterize how carbon is partitioned among different pathways, providing us an opportunity for testing model performance. Our study suggested an overestimation of BPE by most models in natural ecosystems. That is to say, in current models, the fraction of carbon sequestrated by plants allocated to BP is overestimated, but less for respiration purpose. As current models have similar structures in representing photosynthesis, they differ greatly in simulating R_a. R_a is usually separated into two components: growth (R_g) and maintenance respiration (R_m; Atkin, Meir, & Turnbull, 2014; Dewar, Medlyn, & Mcmurtrie, 1999; Gifford, 2003; Ryan et al., 1995; Thornley & Cannell, 2000). This concept has been widely utilized in carbon cycle models, where R_m is first predicted as a function of temperature and biomass, and R_g is a fixed proportion of productivity (Cox, 2001; Piao et al., 2010). The simulations and parameterizations of R_m and R_g vary greatly among models, for instance, constant growth respiration coefficient in CLM is 0.3 (Lawrence et al., 2011), but in TEM6 is 0.2 (Hayes et al., 2011), potentially resulting in large biases of BPE outputs.

Whether a model has an explicit consideration of carbon–nitrogen interaction appears to strongly influence modeled BPE values. Although carbon cycle models overestimate plant BPE, models without carbon–nitrogen interactions show much more model–data mismatch. These models, without a consideration of nitrogen limitation on carbon cycle, may overestimate the CO_2 fertilization effect of vegetation growth and therefore overestimate plant BPE (Vitousek & Howarth, 1991). As for models with carbon–nitrogen interactions, although modeled BPE is smaller than that in carbon-only models and better match with the benchmark (Figure 3a), this does not imply that carbon–nitrogen models perform better, because if modeled GPP and BP are both well simulated, R_a in the model will have to compensate for ignoring the production of nonstructural compounds, and probably overestimating R_a in this case. If the production of nonstructural compounds is incorporated in modeling processes, simulated R_a will have to be (objectively or inadvertently) tuned down. Thus, the processes related to BPE still need improvements in carbon–nitrogen models. This BPE case study also warns that future model development should avoid parameters over-tuning for "perfect" model performance when there are key processes missing yet in models, to generate the right causality in carbon cycle processes and vegetation dynamics.

4.2 | Implications of overestimated BPE in models

As shown in Figure 3a, global BP (excluding cropland) ranges from 35 Pg C/year in CLM4VIC to 88 Pg C/year in SiB3. Since most models overestimate BPE, they most likely also overestimate BP (in case of similar or overestimated global GPP in models). To test this hypothesis, we quantify global natural vegetation BP (excluding cropland) by multiplying the constrained estimate of BPE presented above by observation-based GPP estimates from three different products: the MODIS GPP product (Zhao et al., 2005), a eddy covariance flux tower data-driven GPP product (Jung et al., 2011), and a new GPP product derived by Breathing Earth System Simulator (Jiang & Ryu, 2016)—all averaged over non-cropland vegetation only. The result shows a global BP (excluding cropland) of about 41 ± 6 Pg C/year which is lower by 24 ± 11% than that originally simulated by the models (10 of 14 models; Figure 3).

The overestimation of BPE and BP by carbon cycle models implies reduced carbon storage change during the historical period in models, because carbon storage change is controlled by BP changes and by the turnover rate of ecosystem carbon pools (Luo et al., 2003; Parton, Schimel, Cole, & Ojima, 1987; Potter et al., 1993; Xia, Luo, Wang, & Hararuk, 2013). By correcting the MsTMIP model outputs for their bias of BPE based on equations for substitute models (see Materials and Methods) and not accounting for BPE change in response to climate and rising CO_2 (see Figure S5), we found that the lower BPE implies a 67% smaller increase of

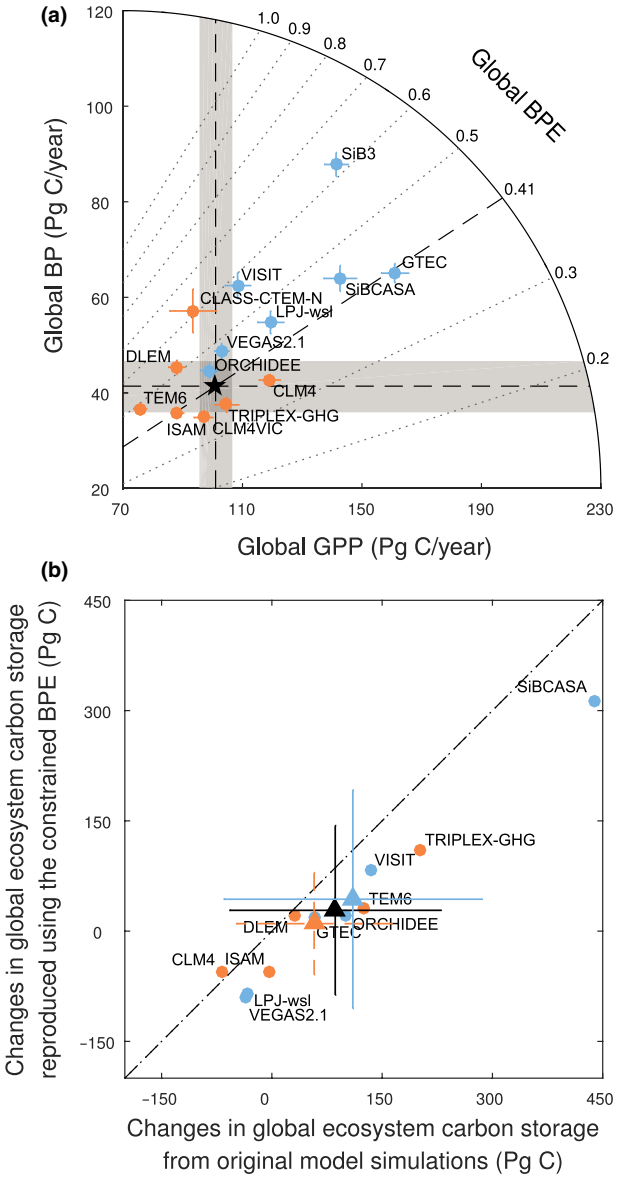

FIGURE 3 Global biomass production (BP) and change in global ecosystem carbon storage during 1901–2010 (excluding cropland). (a) Estimates of GPP, biomass production efficiency (BPE), and BP expressed as the dots in the space, with each represents a model. The black star represents the reference values (i.e., the observation-based estimate of GPP, data-constrained BPE and newly estimated global BP). Shaded gray areas are the uncertainty ranges of the referenced GPP and BP. The uncertainty bars for BP and GPP for the models represent the standard deviations for 1981–2010. (b) Change in global terrestrial carbon storage from 1901 to 2010 estimated by original MsTMIP model simulations and by collecting the mean bias of BPE derived from the MsTMIP models using constrained BPE. The black triangle represents the mean value of all models, and the orange and blue triangles represent the mean values of C-N coupled and C-only models, respectively. The uncertainty bars for the triangles are the standard deviations between models. The solid and dashed bars indicate significant ($p < .05$) and marginally significant ($0.05 < p < .10$) differences, respectively, between the original and the reproduced results. Orange and blue dots in both panels represent C-N coupled and C-only models, respectively

ecosystem carbon storage during 1901–2010 (from 86 ± 144 Pg C of increase in average ecosystem carbon storage in original model simulations to 28 ± 115 Pg C of increase in average ecosystem carbon storage, $p < .01$, Figure 3b), assuming unchanged carbon turnover rate. This overestimation of ecosystem carbon storage increase due to the bias of BPE is particularly significant for carbon-only models ($p < .01$, Figure 3b). Compared to carbon-only models, models with carbon–nitrogen generally reproduce smaller ecosystem carbon storage changes with original model simulations ($p = .09$, Figure 3b), because their BPE is more comparable with the constrained BPE.

In summary, our results show that carbon cycle models generally overestimate BPE, not only suggesting that the capability of future terrestrial carbon sequestration is less than current model predictions but also implying that future reduction of greenhouse gas emission to meet climate target may be underestimated. Furthermore, models with carbon–nitrogen interactions simulate BPE closer to observed values compared to carbon-only models, although R_a in these models is probably overestimated to compensate for the omission of nonstructural carbon fluxes. These results suggest that more efforts should be put into improving carbon cycle modeling with processes treated either very simplistically or insufficiently, in order to represent correct carbon cycle processes and vegetation dynamics for correct reasons. Measurements of BPE across different vegetation types, for different management intensities and different levels of soil-available nitrogen and phosphorus are also needed to refine the global estimation of this key carbon cycle variable.

ACKNOWLEDGEMENTS

This study was supported by the National Key Research and Development Program of China (2016YFC0500203 and 2016YFA0600202), and the National Natural Science Foundation of China (grant numbers 41722101, 41701089 and 41671079), and. P.C., I.J. and J.P. acknowledges support from the European Research Council Synergy grant ERC-2013-SyG-610028 IMBALANCE-P. We thank Multi-scale Synthesis and Terrestrial Model Intercomparison Project (MsTMIP) providing simulation results.

CONFLICT OF INTEREST

The authors declare no competing financial interests.

ORCID

Shushi Peng https://orcid.org/0000-0001-5098-726X
Yongwen Liu https://orcid.org/0000-0002-9664-303X
Atul K. Jain https://orcid.org/0000-0002-4051-3228
Sara Vicca https://orcid.org/0000-0001-9812-5837
Qiuan Zhu https://orcid.org/0000-0002-2246-6325

REFERENCES

Atkin, O. K., Meir, P., & Turnbull, M. H. (2014). Improving representation of leaf respiration in large-scale predictive climate-vegetation models. *New Phytologist*, *202*(3), 743–748. https://doi.org/10.1111/nph.12686

Badgley, G., Field, C. B., & Berry, J. A. (2017). Canopy near-infrared reflectance and terrestrial photosynthesis. *Science Advances*, *3*(3), e1602244. https://doi.org/10.1126/sciadv.1602244

Beer, C., Reichstein, M., Tomelleri, E., Ciais, P., Jung, M., Carvalhais, N., … Papale, D. (2010). Terrestrial gross carbon dioxide uptake: Global distribution and covariation with climate. *Science*, *329*(5993), 834–838. https://doi.org/10.1126/science.1184984

Campioli, M., Vicca, S., Luyssaert, S., Bilcke, J., Ceschia, E., Chapin Iii, F. S., … Janssens, I. A. (2015). Biomass production efficiency controlled by management in temperate and boreal ecosystems. *Nature Geoscience*, *8*(11), 843–846. https://doi.org/10.1038/ngeo2553

Chapin, F. S., Woodwell, G. M., Randerson, J. T., Rastetter, E. B., Lovett, G. M., Baldocchi, D. D., Wirth, C. (2006). Reconciling carbon-cycle concepts, terminology, and methods. *Ecosystems*, *9*(7), 1041–1050.

Ciais, P., Sabine, C., Bala, G., Bopp, L., Brovkin, V., Canadell, J., … Jones, C. (2013). *Carbon and other biogeochemical cycles. Climate change 2013: The physical science basis. Contribution of working group I to the fifth assessment report of the intergovernmental panel on climate change* (pp. 465–570). Cambridge, UK and New York, NY: Cambridge University Press.

Cox, P. M. (2001). Description of the "TRIFFID" dynamic global vegetation model. *Hadley Centre Technical Note*, *24*, 1–16.

Cox, P. M., Pearson, D., Booth, B. B., Friedlingstein, P., Huntingford, C., Jones, C. D., & Luke, C. M. (2013). Sensitivity of tropical carbon to climate change constrained by carbon dioxide variability. *Nature*, *494*(7437), 341–344. https://doi.org/10.1038/nature11882

Cramer, W., Bondeau, A., Woodward, F. I., Prentice, I. C., Betts, R. A., Brovkin, V., … Kucharik, C. (2001). Global response of terrestrial ecosystem structure and function to CO_2 and climate change: Results from six dynamic global vegetation models. *Global Change Biology*, *7*(4), 357–373.

Dewar, R. C., Medlyn, B. E., & Mcmurtrie, R. E. (1999). Acclimation of the respiration/photosynthesis ratio to temperature: Insights from a model. *Global Change Biology*, *5*(5), 615–622. https://doi.org/10.1046/j.1365-2486.1999.00253.x

Erb, K.-H., Fetzel, T., Plutzar, C., Kastner, T., Lauk, C., Mayer, A., … Haberl, H. (2016). Biomass turnover time in terrestrial ecosystems halved by land use. *Nature Geoscience*, *9*(9), 674–678. https://doi.org/10.1038/ngeo2782

Eyring, V., Cox, P. M., Flato, G. M., Gleckler, P. J., Abramowitz, G., Caldwell, P., … Williamson, M. S. (2019). Taking climate model evaluation to the next level. *Nature Climate Change*, *9*, 102–110. https://doi.org/10.1038/s41558-018-0355-y

Fernández-Martínez, M., Vicca, S., Janssens, I. A., Sardans, J., Luyssaert, S., Campioli, M., … Peñuelas, J. (2014). Nutrient availability as the key regulator of global forest carbon balance. *Nature Climate Change*, *4*(6), 471–476. https://doi.org/10.1038/nclimate2177

Fick, S. E., & Hijmans, R. J. (2017). WorldClim 2: New 1-km spatial resolution climate surfaces for global land areas. *International Journal of Climatology*, *37*(12), 4302–4315. https://doi.org/10.1002/joc.5086

Friedlingstein, P., Cox, P., Betts, R., Bopp, L., von Bloh, W., Brovkin, V., … Bala, G. (2006). Climate-carbon cycle feedback analysis: Results from the C4MIP model intercomparison. *Journal of Climate*, *19*(14), 3337–3353.

Friend, A. D., Lucht, W., Rademacher, T. T., Keribin, R., Betts, R., Cadule, P., … Ito, A. (2014). Carbon residence time dominates uncertainty in terrestrial vegetation responses to future climate and atmospheric CO_2. *Proceedings of the National Academy of Sciences of the United States of America*, *111*(9), 3280–3285.

Gifford, R. M. (1995). Whole plant respiration and photosynthesis of wheat under increased CO_2 concentration and temperature: Long-term vs. short-term distinctions for modelling. *Global Change Biology*, *1*(6), 385–396. https://doi.org/10.1111/j.1365-2486.1995.tb00037.x

Gifford, R. M. (2003). Plant respiration in productivity models: Conceptualisation, representation and issues for global terrestrial carbon-cycle research. *Functional Plant Biology*, *30*(2), 171–186. https://doi.org/10.1071/FP02083

Guanter, L., Zhang, Y., Jung, M., Joiner, J., Voigt, M., Berry, J. A., … Griffis, T. J. (2014). Global and time-resolved monitoring of crop photosynthesis with chlorophyll fluorescence. *Proceedings of the National Academy of Sciences of the United States of America*, *111*(14), E1327–E1333. https://doi.org/10.1073/pnas.1320008111

Haberl, H., Erb, K. H., Krausmann, F., Gaube, V., Bondeau, A., Plutzar, C., … Fischer-Kowalski, M. (2007). Quantifying and mapping the human appropriation of net primary production in earth's terrestrial ecosystems. *Proceedings of the National Academy of Sciences of the United States of America*, *104*(31), 12942–12947. https://doi.org/10.1073/pnas.0704243104

Hayes, D. J., McGuire, A. D., Kicklighter, D. W., Gurney, K. R., Burnside, T. J., & Melillo, J. M. (2011). Is the northern high-latitude land-based CO_2 sink weakening? *Global Biogeochemical Cycles*, *25*(3).

Huang, M., Ray, J., Hou, Z., Ren, H., Liu, Y., & Swiler, L. (2016). On the applicability of surrogate-based Markov chain Monte Carlo-Bayesian inversion to the Community Land Model: Case studies at flux tower sites. *Journal of Geophysical Research: Atmospheres*, *121*(13), 7548–7563.

Huntzinger, D. N., Schwalm, C., Michalak, A. M., Schaefer, K., King, A. W., Wei, Y., … Zhu, Q. (2013). The North American carbon program multi-scale synthesis and terrestrial model intercomparison project-part 1: Overview and experimental design. *Geoscientific Model Development*, *6*(6), 2121–2133. https://doi.org/10.5194/gmd-6-2121-2013

Jiang, C., & Ryu, Y. (2016). Multi-scale evaluation of global gross primary productivity and evapotranspiration products derived from Breathing Earth System Simulator (BESS). *Remote Sensing of Environment*, *186*, 528–547. https://doi.org/10.1016/j.rse.2016.08.030

Jung, M., Henkel, K., Herold, M., & Churkina, G. (2006). Exploiting synergies of global land cover products for carbon cycle modeling. *Remote Sensing of Environment*, *101*(4), 534–553. https://doi.org/10.1016/j.rse.2006.01.020

Jung, M., Reichstein, M., Margolis, H. A., Cescatti, A., Richardson, A. D., Arain, M. A., … Gianelle, D. (2011). Global patterns of land-atmosphere fluxes of carbon dioxide, latent heat, and sensible heat derived from eddy covariance, satellite, and meteorological observations. *Journal of Geophysical Research: Biogeosciences*, *116*(G3).

Krinner, G., Viovy, N., de Noblet-Ducoudré, N., Ogée, J., Polcher, J., Friedlingstein, P., Prentice, I. C. (2005). A dynamic global vegetation model for studies of the coupled atmosphere-biosphere system. *Global Biogeochemical Cycles*, *19*(1), https://doi.org/10.1029/2003GB002199

Kwiatkowski, L., Bopp, L., Aumont, O., Ciais, P., Cox, P. M., Laufkötter, C., … Séférian, R. (2017). Emergent constraints on projections of declining primary production in the tropical oceans. *Nature Climate Change*, *7*(5), 355–358. https://doi.org/10.1038/nclimate3265

Landsberg, J. J., & Waring, R. H. (1997). A generalised model of forest productivity using simplified concepts of radiation-use efficiency, carbon balance and partitioning. *Forest Ecology and Management*, *95*(3), 209–228. https://doi.org/10.1016/S0378-1127(97)00026-1

Lawrence, D. M., Oleson, K. W., Flanner, M. G., Thornton, P. E., Swenson, S. C., Lawrence, P. J., … Bonan, G. B. (2011). Parameterization improvements and functional and structural advances in version 4 of the community land model. *Journal of Advances in Modeling Earth Systems*, *3*(1).

Le Quéré, C., Moriarty, R., Andrew, R. M., Canadell, J. G., Sitch, S., Korsbakken, J. I., … Zeng, N. (2015). Global carbon budget 2015. *Earth System Science Data*, *7*, 349–396. https://doi.org/10.5194/essd-7-349-2015

Li, X., Li, Y., Chen, A., Gao, M., Slette, I. J., & Piao, S. (2019). The impact of the 2009/2010 drought on vegetation growth and terrestrial carbon balance in Southwest China. *Agricultural and Forest Meteorology*, *269*, 239–248.

Liu, Y., Piao, S., Gasser, T., Ciais, P., Yang, H., Wang, H., … Wang, K. (2019). Field-experiment constraints on the enhancement of the terrestrial carbon sink by CO fertilization. *Nature Geoscience*. https://doi.org/10.1038/s41561-019-0436-1

Luo, Y., Ahlström, A., Allison, S. D., Batjes, N. H., Brovkin, V., Carvalhais, N., … Zhou, T. (2016). Toward more realistic projections of soil carbon dynamics by Earth system models. *Global Biogeochemical Cycles*, *30*(1), 40–56. https://doi.org/10.1002/2015GB005239

Luo, Y., White, L. W., Canadell, J. G., DeLucia, E. H., Ellsworth, D. S., Finzi, A., Schlesinger, W. H. (2003). Sustainability of terrestrial carbon sequestration: A case study in Duke Forest with inversion approach. *Global Biogeochemical Cycles*, *17*(1), https://doi.org/10.1029/2002GB001923

Luyssaert, S., Inglima, I., Jung, M., Richardson, A. D., Reichstein, M., Papale, D., … Aragao, L. E. O. C. (2007). CO_2 balance of boreal, temperate, and tropical forests derived from a global database. *Global Change Biology*, *13*(12), 2509–2537.

McCree, K. J., & Troughton, J. H. (1966). Prediction of growth rate at different light levels from measured photosynthesis and respiration rates. *Plant Physiology*, *41*(4), 559–566. https://doi.org/10.1104/pp.41.4.559

Nemani, R., Hashimoto, H., Votava, P., Melton, F., Wang, W., Michaelis, A., … White, M. (2009). Monitoring and forecasting ecosystem dynamics using the Terrestrial Observation and Prediction System (TOPS). *Remote Sensing of Environment*, *113*(7), 1497–1509. https://doi.org/10.1016/j.rse.2008.06.017

Parton, W. J., Schimel, D. S., Cole, C. V., & Ojima, D. S. (1987). Analysis of factors controlling soil organic matter levels in Great Plains Grasslands. *Soil Science Society of America Journal*, *51*(5), 1173–1179.

Peel, M. C., Finlayson, B. L., & McMahon, T. A. (2007). Updated world map of the Köppen-Geiger climate classification. *Hydrology and Earth System Sciences Discussions*, *4*(2), 439–473. https://doi.org/10.5194/hessd-4-439-2007

Peng, C., Liu, J., Dang, Q., Apps, M. J., & Jiang, H. (2002). TRIPLEX: A generic hybrid model for predicting forest growth and carbon and nitrogen dynamics. *Ecological Modelling*, *153*(1–2), 109–130. https://doi.org/10.1016/S0304-3800(01)00505-1

Peñuelas, J., Ciais, P., Canadell, J. G., Janssens, I. A., Fernández-Martínez, M., Carnicer, J., … Sardans, J. (2017). Shifting from a fertilization-dominated to a warming-dominated period. *Nature Ecology & Evolution*, *1*(10), 1438–1445. https://doi.org/10.1038/s41559-017-0274-8

Piao, S., Ciais, P., Friedlingstein, P., Peylin, P., Reichstein, M., Luyssaert, S., … Vesala, T. (2008). Net carbon dioxide losses of northern ecosystems in response to autumn warming. *Nature*, *451*(7174), 49–52. https://doi.org/10.1038/nature06444

Piao, S., Huang, M., Liu, Z., Wang, X., Ciais, P., Canadell, J. G., … Wang, T. (2018). Lower land-use emissions responsible for increased net land carbon sink during the slow warming period. *Nature Geoscience*, *11*(10), 739–743. https://doi.org/10.1038/s41561-018-0204-7

Piao, S., Luyssaert, S., Ciais, P., Janssens, I. A., Chen, A., Cao, C., … Wang, S. (2010). Forest annual carbon cost: A global-scale analysis of autotrophic respiration. *Ecology*, *91*(3), 652–661. https://doi.org/10.1890/08-2176.1

Piao, S., Sitch, S., Ciais, P., Friedlingstein, P., Peylin, P., Wang, X., … Huntingford, C. (2013). Evaluation of terrestrial carbon cycle models for their response to climate variability and to CO_2 trends. *Global Change Biology*, *19*(7), 2117–2132.

Potter, C. S., Randerson, J. T., Field, C. B., Matson, P. A., Vitousek, P. M., Mooney, H. A., & Klooster, S. A. (1993). Terrestrial ecosystem production: A process model based on global satellite and surface data. *Global Biogeochemical Cycles*, *7*(4), 811–841. https://doi.org/10.1029/93GB02725

Rogers, A., Medlyn, B. E., Dukes, J. S., Bonan, G., von Caemmerer, S., Dietze, M. C., … Zaehle, S. (2017). A roadmap for improving the representation of photosynthesis in Earth system models. *New Phytologist*, *213*(1), 22–42. https://doi.org/10.1111/nph.14283

Ryan, M. G., Gower, S. T., Hubbard, R. M., Waring, R. H., Gholz, H. L., Cropper, W. P., & Running, S. W. (1995). Woody tissue maintenance respiration of four conifers in contrasting climates. *Oecologia*, *101*(2), 133–140. https://doi.org/10.1007/BF00317276

Sands, P. J., Battaglia, M., & Mummery, D. (2000). Application of process-based models to forest management: Experience with PROMOD, a simple plantation productivity model. *Tree Physiology*, *20*(5–6), 383–392. https://doi.org/10.1093/treephys/20.5-6.383

Sargsyan, K., Safta, C., Najm, H. N., Debusschere, B. J., Ricciuto, D., & Thornton, P. (2014). Dimensionality reduction for complex models via Bayesian compressive sensing. *International Journal for Uncertainty Quantification*, *4*(1), 63–93. https://doi.org/10.1615/Int.J.UncertaintyQuantification.2013006821

Thornley, J. H. M., & Cannell, M. G. R. (2000). Modelling the components of plant respiration: Representation and realism. *Annals of Botany*, *85*(1), 55–67.

Tian, H., Chen, G., Zhang, C., Liu, M., Sun, G. E., Chappelka, A., … Vance, E. (2012). Century-scale responses of ecosystem carbon storage and flux to multiple environmental changes in the southern United States. *Ecosystems*, *15*(4), 674–694. https://doi.org/10.1007/s10021-012-9539-x

Veroustraete, F., Sabbe, H., & Eerens, H. (2002). Estimation of carbon mass fluxes over Europe using the C-Fix model and Euroflux data. *Remote Sensing of Environment*, *83*(3), 376–399. https://doi.org/10.1016/S0034-4257(02)00043-3

Vicca, S., Luyssaert, S., Peñuelas, J., Campioli, M., Chapin, F. S. III, Ciais, P., … Janssens, I. A. (2012). Fertile forests produce biomass more efficiently. *Ecology Letters*, *15*(6), 520–526. https://doi.org/10.1111/j.1461-0248.2012.01775.x

Vitousek, P. M., & Howarth, R. W. (1991). Nitrogen limitation on land and in the sea: How can it occur? *Biogeochemistry*, *13*(2), 87–115. https://doi.org/10.1007/BF00002772

Waring, R. H., Landsberg, J. J., & Williams, M. (1998). Net primary production of forests: A constant fraction of gross primary production? *Tree Physiology*, *18*(2), 129–134. https://doi.org/10.1093/treephys/18.2.129

Wei, Y., Liu, S., Huntzinger, D. N., Michalak, A. M., Viovy, N., Post, W. M., … Shi, X. (2014). The North American carbon program multi-scale synthesis and terrestrial model intercomparison project-Part 2: Environmental driver data. *Geoscientific Model Development Discussions*, *7*, 2875–2893. https://doi.org/10.5194/gmd-7-2875-2014

Wenzel, S., Cox, P. M., Eyring, V., & Friedlingstein, P. (2014). Emergent constraints on climate-carbon cycle feedbacks in the CMIP5 Earth system models. *Journal of Geophysical Research: Biogeosciences*, *119*(5), 794–807. https://doi.org/10.1002/2013JG002591

Xia, J., Luo, Y., Wang, Y. P., & Hararuk, O. (2013). Traceable components of terrestrial carbon storage capacity in biogeochemical models. *Global Change Biology*, *19*(7), 2104–2116. https://doi.org/10.1111/gcb.12172

Yao, Y., Piao, S., & Wang, T. (2018). Future biomass carbon sequestration capacity of Chinese forests. *Science Bulletin*, *63*(17), 1108–1117. https://doi.org/10.1016/j.scib.2018.07.015

Zhang, Y., Xu, M., Chen, H., & Adams, J. (2009). Global pattern of NPP to GPP ratio derived from MODIS data: Effects of ecosystem type, geographical location and climate. *Global Ecology and Biogeography*, *18*(3), 280–290. https://doi.org/10.1111/j.1466-8238.2008.00442.x

Zhang, Y., Yu, G., Yang, J., Wimberly, M. C., Zhang, X. Z., Tao, J., … Zhu, J. (2014). Climate-driven global changes in carbon use efficiency. *Global*

Ecology and Biogeography, *23*(2), 144–155. https://doi.org/10.1111/geb.12086

Zhao, C., Piao, S., Wang, X., Huang, Y., Ciais, P., Elliott, J., … Peñuelas, J. (2016). Plausible rice yield losses under future climate warming. *Nature Plants*, *3*(1). https://doi.org/10.1038/nplants.2016.202

Zhao, M., Heinsch, F. A., Nemani, R. R., & Running, S. W. (2005). Improvements of the MODIS terrestrial gross and net primary production global data set. *Remote Sensing of Environment*, *95*(2), 164–176. https://doi.org/10.1016/j.rse.2004.12.011

Zhu, Q., Liu, J., Peng, C., Chen, H., Fang, X., Jiang, H., … Zhou, X. (2014). Modelling methane emissions from natural wetlands by development and application of the TRIPLEX-GHG model. *Geoscientific Model Development*, *7*(3), 981–999. https://doi.org/10.5194/gmd-7-981-2014

SUPPORTING INFORMATION

Additional supporting information may be found online in the Supporting Information section at the end of the article.

How to cite this article: He Y, Peng S, Liu Y, et al. Global vegetation biomass production efficiency constrained by models and observations. *Glob Change Biol*. 2019;00:1–11. https://doi.org/10.1111/gcb.14816